NUMERICAL SIMULATION OF POLYPROPYLENE AND FIBER REINFORCED POLYMER COMPOSITE RETROFITTED MASONRY WALLS

Saleem M. Umair[1], Muneyoshi NUMADA[2] and Kimiro MEGURO[3]

ABSTRACT: In this study, an attempt is made to numerically simulate the behavior of Fiber Reinforced Polymer (FRP) and Polypropylene (PP) band composite using the Applied Element Method (AEM). Both of these materials have their own unique properties. FRP is used to increase the strength, whereas PP-band is used to increase the deformation capacity and energy dissipation capacity of masonry wall system. Behavior of these materials is numerically modeled by modifying AEM using various constitutive laws proposed in latest research works. In order to verify the numerical results an experimental study is also carried out. Proposed numerical tool has shown a good agreement with experimental results.

Key Words: Applied Element Method, FRP and PP-band composite, Seismic retrofitting, Energy dissipation capacity

INTRODUCTION

Unreinforced masonry (URM) structures have suffered extensive damage during earthquakes, such as the 1997 Umbria-Marche, Italy, the 2001 Bhuj, India, the 2003 Bam, Iran, the 2005 Kashmir, Pakistan and the 2008 Wenchuan, China earthquakes have shown the collapse of larger number of masonry structures especially in areas of poorly designed and constructed houses. Therefore, retrofitting of low earthquake-resistant masonry structures is the key issue for earthquake disaster reduction of both structures and human causalities (Meguro and Mayorca 2005). Additionally, seismic retrofitting reduces the costs of rescue and first aid activities, rubble removal, temporary shelter preparation and permanent residential reconstruction to re-establish normal daily life (Yoshimura and Meguro 2004).

URM buildings can fail due to deficient strength of the walls when loaded in-plane but weak out-of-plane behavior is the major cause of collapse of masonry structures. In order to avoid out of plane failure of masonry walls different retrofitting procedures has been adopted by different researchers. Some of the retrofitting methods include the seismic retrofit of URM walls using externally-bonded or near surface mounted Fiber Reinforced Polymer (FRP) laminates, FRP bars and fabrics. FRP has some well-known advantages over conventional retrofitting techniques such as high strength, ease of application, corrosion resistance and high strength to weight ratio. FRP retrofitting methods can increase the structural strength but make failure brittle. Therefore, FRP retrofitted walls collapses suddenly unless the whole masonry wall is fully wrapped by FRP whose cost may become sometimes larger than that of masonry construction.

Along with above retrofitted methods, Meguro and Mayorca (Meguro and Mayorca 2005) have

[1] Graduate Student, The University of Tokyo
[2] Research Associate, ICUS, IIS, The University of Tokyo
[3] Director/Professor, ICUS, IIS, The University of Tokyo

developed polypropylene band (PP-band) retrofitting method considering economic affordability, local acceptability, material availability and technological applicability required for retrofitting. PP-band is a very cheap material with fairly large deformation capacity. Main objective of PP-band retrofitting is to hold the masonry components into a single unit and to prevent the collapse of masonry structure. After carrying out a series of experiments ranging from small-scale model to full-scale masonry house, it was found that PP-band retrofitted walls can withstand much stronger input ground motion without collapse (Sakthi and Meguro 2008).

In this study, we proposed a new composite retrofitting method for URM structures. An attempt has been made to find a composite material using FRP and PP-band which can increase not only the structural strength but also the deformation capacity of masonry by combining strongpoints of both methods. In order to achieve aforementioned objectives, the research is divided into two parts: modification of existing Applied Element Method (AEM) for numerical simulation of FRP+PP-band composite and experimental verification of modified numerical tool.

MODIFIED THREE DIMENSSIONAL APPLIED ELEMENT METHOD

Applied Element Method (AEM)

The AEM was originally developed by Kimiro Meguro and Hatem Tagel din (Meguro and Tagle din 2001) and it is a derivative of Finite Element Method and Discrete Element Method. The AEM was initially used for analysis of linear and non-linear behavior of reinforced concrete structures. Application of the AEM for masonry structures unretrofitted and PP-band retrofitted is further enhanced by Meguro and Mayorca (Meguro and Mayorca 2003). In the AEM masonry wall system is divided into distinct rigid elements mainly carrying the mass and damping. Elements are joined together with the help of shear and normal springs.. Heterogeneous behavior of masonry structures was covered by Guaragian and Meguro (Guaragian and Meguro 2006) using constitutive laws of masonry proposed by Gamaraotta (Gamaraotta 1997). To simulate three dimensional behavior of masonry structures, Kawin and Meguro (Kawin and Meguro 2008) modified all the two dimension system of analysis to three dimensional analysis systems keeping same theoretical background.

Three dimensional grid system of masonry wall is defined based upon the size of wall, time and storage of analyzing machine, level of information required and efficiency. All elements are connected to each other with normal and shear springs. Following Equations 1 and 2 give normal stiffness K_n and shear stiffness K_s of normal and shear springs respectively.

$$K_n = \frac{E_b \times b \times c}{a} \tag{1}$$

$$K_{S1,S2} = \frac{G_b \times b \times c}{a} \tag{2}$$

Where a ,b, c are length, width and height of element; E_b = Young's modulus of brick element; G_b = shear modulus of brick element; a = length of element; b = width of element, and c = height of element. Arrangement and connectivity of elements is shown in Figs. 1(a), 1(b) and 1(c). Figure 1(a) shows arrangement of masonry elements and Figure 1(b) shows the connectivity of two same types of elements at brick to brick element interface.

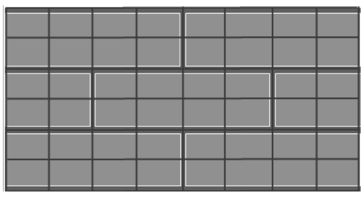

(a) Arrangement of elements in masonry wall system

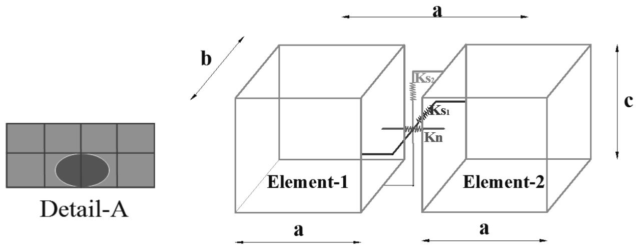

(b) Connectivity of two elements at brick to brick interface

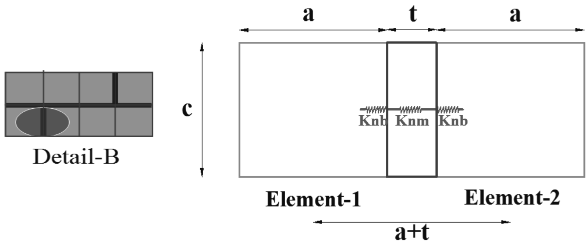

(c) Connectivity of two elements at brick to mortar interface

Figure 1. Arrangement of masonry elements in masonry wall system and their spring connectivity

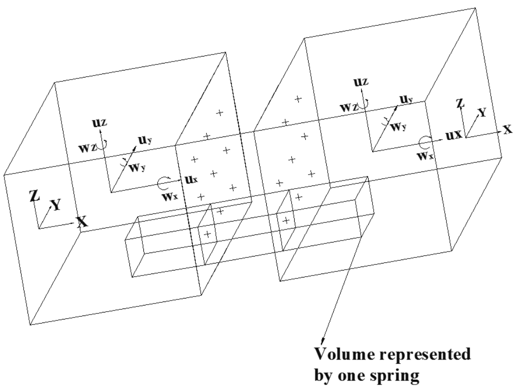

Figure 2. Degree of freedom of individual elements and their springs on connected face

Connectivity of brick to mortar spring is shown in Fig. 1(c). Stiffness of brick to mortar springs is computed by assuming a system in which brick and mortar springs are in series which enables us to calculate the equivalent normal and shear stiffness. Following Equations 3 to 6 give brick to mortar spring normal and shear stiffness. A three dimensional view of connected elements and their nodal degree of freedom is also shown in Figure 2.

$$\frac{1}{K_{n,eq}} = \frac{1}{K_{nb}} + \frac{1}{K_{nm}} \tag{3}$$

$$\frac{1}{K_{n,eq}} = \frac{a-t}{E_b \times b \times c} + \frac{t}{E_m \times b \times c} \tag{4}$$

$$\frac{1}{K_{s1,eq}} = \frac{a-t}{G_b \times b \times c} + \frac{t}{G_m \times b \times c} \tag{5}$$

$$\frac{1}{K_{s2,eq}} = \frac{a-t}{G_b \times b \times c} + \frac{t}{G_m \times b \times c} \tag{6}$$

where $K_{n,eq}$ = spring equivalent normal stiffness; $K_{s1,eq}$ = spring equivalent shear stiffness in 1 direction; $K_{s2,eq}$ = spring equivalent shear stiffness in 2 direction ; $K_{s2,eq}$ = spring equivalent shear stiffness in 2 direction ; E_m = Youngs Modulus of mortar; G_m = shear modulus of mortar and t = mortar thickness.

Modification for FRP and PP-band Composite in 3D-AEM

Previous version of 3-D AEM was not able to deal with FRP retrofitted wallet as well as FRP and PP-band retrofitted wallet. In order to implement new concept of FRP and PP-band retrofitting technique, it was required to enhance the capacity of existing version to deal with problems of composite retrofitting. Required objectives are achieved by making some major changes in the structure of existing program. FRP can completely change the mode of failure of masonry e.g. from joint sliding to diagonal shear failure. There could be three possible modes of failure when FRP is attached to brick surface with epoxy as follows:

1) FRP and epoxy debonding
2) Brick surface tensile failure
3) FRP rupture

Although ideal case is that FRP reaches its ultimate tensile capacity, but experimental data shows FRP contribution is far less due to premature debonding failure or surface tensile failure of brick. Modeling of FRP in advanced 3D-AEM is achieved by selecting a suitable damage model to compute the shear contribution provided by the FRP. In case of FRP and FRP+PP-band retrofitted masonry wallet, the resulting shear strength of masonry is calculated by Equation 7.

$$V = V_m + V_{FRP} \tag{7}$$

Where V_m = masonry shear strength contribution; V_{FRP} = FRP shear strength contribution.

Gambrotta et al (Gamaraotta 1997) constitutive law has been adopted to simulate non-linear cyclic behavior of the masonry and can reflect well the important physical phenomenon of masonry. For masonry retrofitted with FRP, limited models are developed (Zhuge 2010). All of them are based upon the assumption that shear strength of FRP retrofitted wallet is sum of shear strength provided by masonry and shear strength contribution of FRP. It was a difficult task to find out the most suitable damage model. In this regard, Y. Zhuge (Zhuge 2010) has compared the different damage models of FRP retrofitted walls under in plane shear. According to his finding, Triantafillou (Triantafillou 1998) model has given non-conservative but fairly close estimate of FRP shear strength. Based upon his finding TA model has been adopted to set the failure criterion of FRP by comparing effective FRP strain $\varepsilon_{FRP,e}$ at different load computed by the AEM.

Triantafillou first proposed his model in 1998 which was based upon the assumption that the contribution of vertical FRP is negligible and shear resistance mechanism is only associated with the action of horizontal laminates(Triantafillou 1998). But, this model has not served satisfactory when compared with experimental data. Later Triantafillou and Antonopoulos (Triantafillou and Antonopoulos 2000) revised the previous model and proposed an improved one. He proposed three expressions to distinguish FRP debonding, rupture and type of FRP materials. Equation 8 below gives the FRP and epoxy strain along with the limiting FRP ratio.

(a) Strain in FRP

$$\varepsilon_{f,e} = 0.17\left(\frac{f_c^{\,2/3}}{E_f \rho_f}\right)^{0.3} \varepsilon_{f,u} \quad 8\,(a)$$

(b) Strain in epoxy

$$\varepsilon_{f,e} = 0.65\left(\frac{f_c^{\,2/3}}{E_f \rho_f}\right)^{0.56} \times 10^{-3}\varepsilon_{f,u} \quad 8(b)$$

(c) Limiting FRP ratio

$$(E_f \rho_f)_{\lim} = \left(\frac{0.65\times 10^{-3}}{\varepsilon_{\max}}\right)^{0.56} f_c^{2/3} \quad 8(c)$$

Bi-linear elastic behavior of PP-band is considered in modified 3D-AEM. PP-band is modeled as beam element having span equal to the length between two intersection points. PP-band is carrying only axial tensile stiffness based upon the nodal connectivity of PP-band with brick surface. PP-band is connected to the masonry with the help of out of plane connectors at specified interval. PP-band mainly contributes in its axial stiffness depending upon the nodal connectivity of band with the brick masonry.

VERIFICATION OF MODIFIED 3D- APPLIED ELEMENT METHOD

A series of experiments are carried out in order to verify the proposed changes in 3D-AEM. Two types of experimental studies are carried out: material test to determine the material properties of PP-band, bricks, mortar, masonry out of plane load test are carried out on 1/4-scaled masonry wallets.

Material tests
Properties of CFRP and epoxy
Properties of CFRP and epoxy are provided by the supplier of these materials. Bi directional type of fiber layout is used in CFRP. Thickness of CFRP sheet is 0.5mm. Bond E-250 epoxy is used to apply CFRP over the brick surface. Tables 1 and 2 show the properties of CFRP and epoxy respectively. All epoxy strength parameters are examined at temperature of 20±1°C after curing time of 7 days.

Table 1 Material properties of CFRP

Material	**Tensile modulus** (GPa)	**Bending strength** (MPa)	**Bending modulus** (GPa)	**Compressive strength** (MPa)	**Ultimate Elongation** (%)
CFRP	120	130	90	900	2

Table 2 Material properties of Epoxy

Material	Tensile strength (MPa)	Tensile shear bond strength (MPa)	Bending strength (MPa)	Compressive strength (MPa)	Compressive shear bond strength (MPa)
Epoxy	20	9.6	45	50	21

Axial tensile test on polypropylene (PP) band

Three sample of PP-band with 6mm×0.6mm in nominal area of cross section and 150mm in gauge length are tested under uniaxial tensile loading using displacement control universal testing machines (UTM). Table 3 shows the tension test results of PP-band.

Table 3 Polypropylene band tension test results

Specimen	Maximum Axial Stress (MPa)	Initial Modulus (GPa)	Residual Modulus (GPa)	Failure Strain (%)
PP-1	254.20	7.38	1.91	12.30
PP-2	246.50	6.95	2.06	12.67
PP-3	234.40	6.42	1.96	11.91
Average	245.03	6.92	1.98	12.29

Test on masonry

Compression, Shear and bond tests are carried out in order to determine the properties of brick, mortar, and masonry. Table 4 shows the properties of different materials used for construction of masonry wallets. Bricks compressive strength is determined according to ASTM C-67. Three samples of burnt brick were tested under direct compression. Three mortar cubes of 50mm×50mm×50mm containing a weight mixed proportion of cement, lime and sand (250g: 1,000g: 2,800g) were tested with 0.25 water/cement ratios according to ASTM C-109. Three samples of brick triplets, each triplet consisting of three bricks joined together by 5 mm mortar thickness were prepared to evaluate the shear strength of masonry units. Three masonry prisms each consisting of five bricks were tested according to ASTM C-1314.

Table 4 Characteristics of materials used in experiments

Test / Specimen	Compressive strength of brick (MPa)	Compressive strength of mortar cube (MPa)	Compressive strength of masonry prism (MPa)	Shear strength of mortar (MPa)	Bond strength of mortar (MPa)
1	25.10	1.08	15.95	0.24	0.0040
2	26.60	1.07	11.60	0.15	0.0050
3	26.70	1.34	13.25	0.21	0.0040
Average	26.10	1.16	13.60	0.20	0.0043

Masonry Wallet Testing Plan

Figure 3 shows four types of masonry wallets. Dimension of masonry wallet is 475mm x 238mm x 50mm. All of these wallets are constructed using 75mm x 37mm x 50mm burnt brick units. Cement lime mortar with a weight mixed proportion of cement, lime and sand

(250g: 1,000g: 2,800g) is made with 0.25 water/cement ratios. Masonry wallets are constructed, cured and tested under same conditions. In case of CFRP and CFRP+PP-band retrofitted masonry wallets, CFRP is pasted on wallet surface with the help of strong epoxy and cured for 24 hours whereas PP-band and CFRP+PP-band retrofitted, PP-band is applied on both faces with the help of ultrasonic welder and also connected in out of plane direction.

Three of the masonry wallets are retrofitted using different retrofitting schemes. One is PP-band retrofitted, one is CFRP retrofitted and one is CFRP+PP-band retrofitted. Two CFRP strips with the dimension 475mm x 40mm x 0.5mm are used on both faces of CFRP and CFRP+PP-band retrofitted masonry wallets. PP- band mesh with the pitch of 50mm is used for PP-band retrofitted and CFRP+PP-band retrofitted masonry wallet.

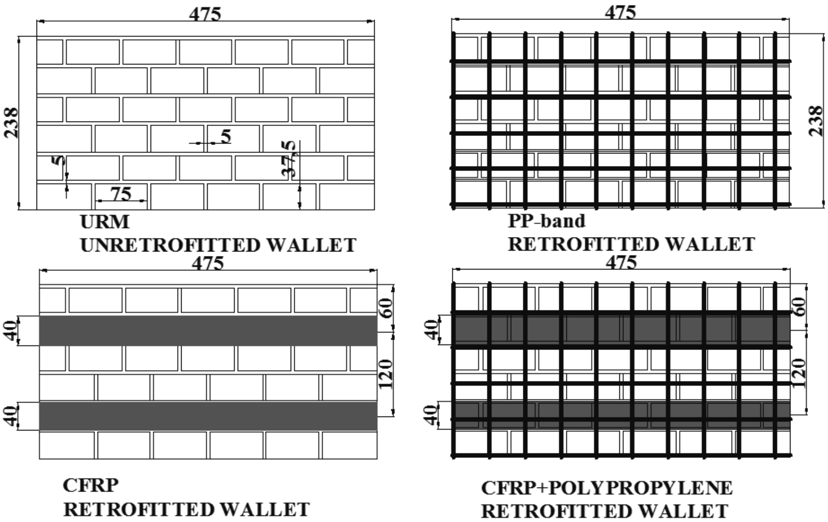

Figure 3. Masonry wallets out of plane testing plan for verification of modified 3D-AEM

RESULTS AND DISCUSSIONS

Four types of masonry wallets were tested and numerically simulated using modified 3D-AEM under out of plane static loading and their load-displacement curves were obtained as shown in Fig 4. Figure 4 shows the comparison of experimental and numerical load-displacements curves of all the masonry wallets. Figure 4(a) shows that experimental and numerical results of non-retrofitted masonry wallets. URM masonry wallets have shown different peak strengths with varying initial stiffness. Numerical results are in close agreement of experimental results. Although, the initial stiffness in case of numerical curve has slight differences but the peak load is almost same as that of experimentally determined. Figure 4(b) shows the numerical and experimental load displacement curves of PP-band retrofitted masonry wallets. Experimental and numerical results are in close range up to the displacement range of 25mm after that numerical stiffness becomes higher. It is because of very high level of uncertainty in terms of interlocking, fixity and arrangement of brick elements during the experiment when subjected to higher displacements. Figure 4(c) mainly shows the comparison of numerical and experimental results of CFRP retrofitted masonry wallet. These two are again in very good arrangement because FRP is totally elastic up to the final failure of masonry wallets. There was some initial drop in experimental results because of separation of one brick layer from masonry wallet. Load displacement comparison of numerical and experimental results of CFRP+PP-band retrofitted is shown in Figure 4(d). CFRP+PP-band retrofitted masonry wallet has different experimental and numerical peak loads but remaining behavior is almost in a close range. Even the experimental peak loads in case of CFRP retrofitted and CFRP+PP-band retrofitted masonry wallet are different for the same quantity of CFRP. The possible reasons for the lower experimental peak strength of CFRP+PP-band retrofitted masonry wallet could be the improper epoxy bonding or poor brick surface conditions.

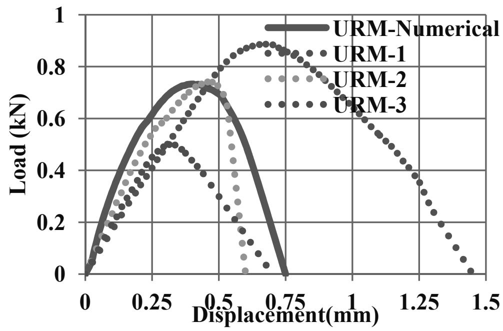

(a) Numerical and experimental load-displacement curves of URM

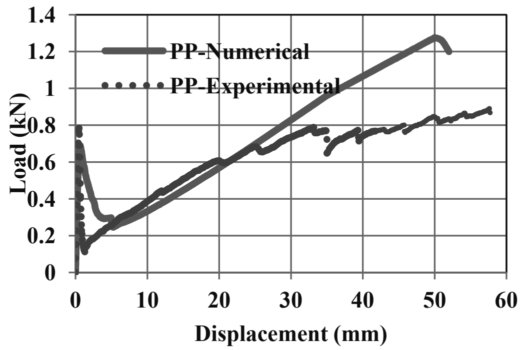

(b) Numerical and experimental load-displacement curves of PP-band retrofitted masonry wallet.

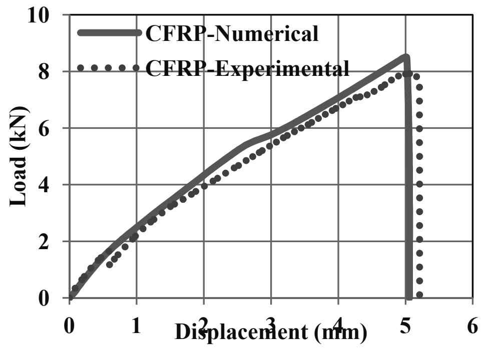

(c) Numerical and experimental load-displacement curves of CFRP retrofitted masonry wallet.

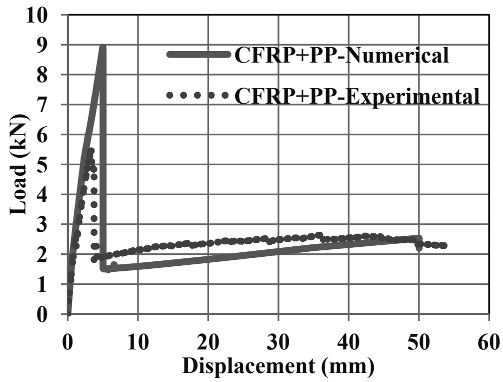

(d) Numerical and experimental load-displacement curves of CFRP+PP-band retrofitted masonry wallet.

Figure 5. Comparison of experimental and numerical load-displacement curves of URM, PP-band, CFRP and CFRP+PP-band retrofitted masonry wallet under out of plane loading

FAILURE MODES

Table 5 shows the graphic comparison of failure modes obtained from experiments and numerical simulation of URM, PP-band, CFRP and CFRP+PP-band retrofitted masonry wallets. Failure patterns in case of URM, PP-band and CFRP+PP retrofitted masonry wallets are very close to each other but in case of CFRP retrofitted masonry wallet, numerical failure mode is different from experimental failure mode. It is because of separation of one complete layer of brick from the masonry wallet. But, in case of CFRP+PP-band retrofitted masonry wallet, separation of this layer of brick was prevented by the holding effect of PP-band and wallet is not defragmented even for a high out of plane displacement range. In case of CFRP and CFRP+PP-band retrofitted masonry wallets, failure is due to delamination of CFRP from the brick surface.

Table 5 Graphic comparison of failure modes of masonry wallets

	Experimental	Numerical
URM	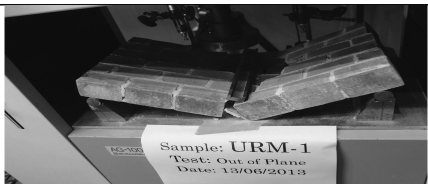	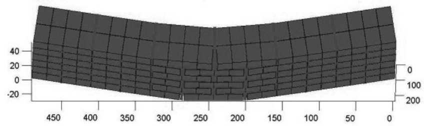
PP-band	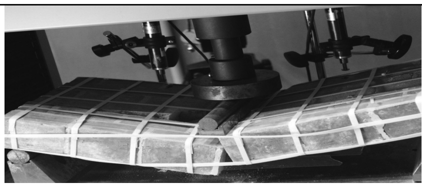	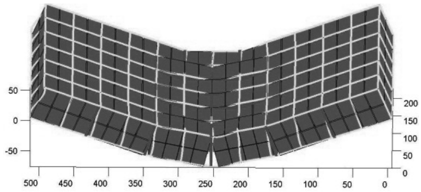
CFRP	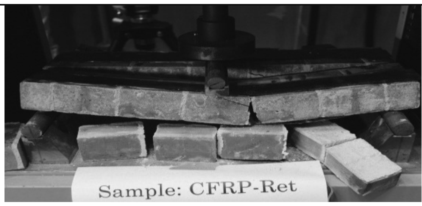	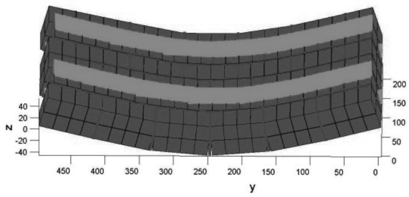
CFRP+PP	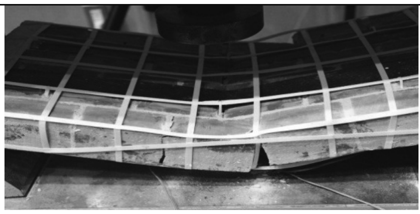	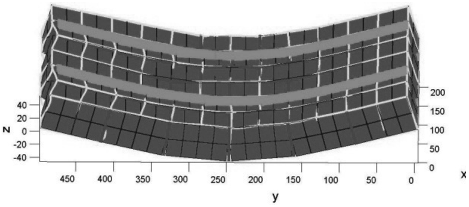

CONCLUSIONS

Based upon the current experimental and numerical study, we can divide conclusions in two main parts consisting of performance of proposed retrofitting scheme and efficiency of the AEM based numerical simulation.

Proposed retrofitting technique is a viable solution of URM retrofitting problems. PP-band has significantly increased the deformation capacity and energy dissipation capacity whereas CFRP-retrofitted wallet has shown significant increase in the initial out of plane strength. CFRP retrofitted wallet has shown a brittle failure. This deficiency of CFRP retrofitted wallet has been overcome by the application of PP-band. CFRP+PP-band retrofitted wallet has not only increased the initial strength but also the deformation capacity and energy dissipation capacity of the masonry wallet.

CFRP+PP-band has not only increased the initial strength but the residual strength of the wallets is also increased.

The AEM is a good tool for analyzing behavior of a non-linear material like masonry in an efficient way. Experimental and numerical results are in close agreement in case of URM, PP-band retrofitted and CFRP retrofitted wallets, whereas CFRP+PP-band retrofitted wallet has shown different peaks. It is because of variation in bonding properties of epoxy and FRP over the wallet surface as initial peak obtained from numerical simulation using CFRP retrofitted one and CFRP+PP-band retrofitted one are similar. In case of PP- band retrofitted wallet, experimental and numerical results are close enough for medium displacement ranges but for large displacements, results are variable. This is because of uncertain rearrangement of elements when subjected to large displacements during the experiment. But in simulation, the failure is independent of interlocking and rearrangement. Failure always starts at those elements where normal and shear springs have reached their capacity and failed propagating redistribution of forces in the residual spring system and this process continues up to final displacement levels.

REFERENCES

Gambrotta L. & Lagomarsino S. (1997). “Damage Model for the Seismic Response of Brick Masonry Shear Walls. Part1: The Mortar Joint Model and its Application.” *Earthquake Engineering and Structural Dynamics,* Vol. 26, 423-439.

Guragain. (2006). “Numerical Simulation of Masonry Structures under Cyclic Loading using Applied Element Method.” *Master Thesis*, Department of Civil Engineering, University of Tokyo, Japan.

Kawin Worakanchana, Paola Mayorca, Ramesh Guragain, Sathiparan Navaratnanaj & Kimiro Meguro. (2008). “3-D Applied Element Method for PP-band Retrofitted Masonry.” *Proc.,* 14th *World Conference on Earthquake Engineering, Beijing, China.*

Kimiro Meguro and Hatem Tagel Din. (2001). “Applied Element simulation of RC Structures under Cyclic Loading.” *Journal of Structural Engineering* , Vol. 127, No. 11, 1295-1305.

Kimiro Meguro, Paola Mayorca, Sathiparan Navaratnanaj, Ramesh. Guragain, & N . Nesheli, (2005). “Shaking Table Tests of 1/4 Scaled Masonry Models Retrofitted with PP-band Meshes.” *Proc., 3rd International Symposium on New Technologies for Urban Safety of Mega Cities in Asia, Singapore,* 9-18.

Miho Yoshimura and Kimiro Meguro. (2004). “Proposal of Retrofitting Promotion System for Low Earthquake-Resistant Structures in Earthquake Prone Countries.” *Proc., 13th World Conference on Earthquake Engineering, Vancouver, Canada,* Vol. 1, Paper No. 927.

Navaratnarajah Sathiparan. (2008). “Experimental study of PP-band mesh seismic retrofitting for low earthquake masonry resisting structures.” *PhD Dissertation*, Department of Civil Engineering, University of Tokyo, Japan.

Paola Mayorca and Kimiro Meguro. (2003). “Proposal of a new economic retrofitting method for masonry structures.” *Proc. of the 27th JSCE Symposium of Earthquake Engineering.*

Triantafillou. T.C. (1998). “Strengthening of Masonry Structures using Epoxy Bonded FRP Laminates.” *Journal of Composite Construction*, Vol. 2 No. 3, 96-104.

Triantafillou T., Antonopoulos C. (2000). “Design of concrete flexural members strengthened in shear with FRP.” *ASCE Journal of Composites for Construction*, Vol. 4, No. 4, 198-205.

Y. Zhuge. (2010). “FRP-Retrofitted URM Walls under in Plane Shear: Review and Assessment of Available Models.” *ASCE Journal of Composites for Construction,* Vol. 14, No. 6, 743-753.

.